Inorganic Chemistry

Article

Imidazole-Substituted Oxoverdazyl Radical As a Mediator of Intramolecular and Intermolecular Exchange Interaction

Lucie Norel,[†] Fabrice Pointillart,[†] Cyrille Train,*,[†] Lise-Marie Chamoreau,[†] Kamal Boubekeur,[†] Yves Journaux,[†] Aaron Brieger,[‡] and David J. R. Brook[§]

Laboratoire de Chimie Inorganique et Matériaux Moléculaires, UMR 7071, IFR 2769, UPMC Univ. Paris 6, case 42, 4 place Jussieu, F75252 Paris cedex 05, France, Department of Chemistry and Biochemistry, University of Detroit Mercy, 4001 W. McNichols Rd, Detroit, Michigan 48221, and Department of Chemistry, San Jose State University, One Washington Square, San Jose, California 95192

The 3-(2′-imidazolyl)-1,5-dimethyl-6-oxoverdazyl radical (imvd•) and the corresponding tetrazane H₃imvd were prepared and structurally characterized, the former as two different hydrates. Reaction of imvd• with [M(hfac)₂] led to the formation of monometallic complexes [M(hfac)₂(imvd•)] (M = Ni and Mn). They were characterized by single-crystal X-ray diffraction. In the solid state, all four radical-containing compounds exhibit imidazole−oxoverdazyl π stacking. Following the structural analysis, imvd• behaves as an antiferromagnetic (AF) coupled chain with $J = -100$ cm^{-1} ($H = -J\sum S_i S_{i+1}$). The magnetic behavior of [M(hfac)₂(imvd•)] complexes is interpreted with a four-coupled spin model with a metal ion radical intramolecular interaction ($J_{Mn} = -62.5$ cm^{-1} and $J_{Ni} = 193$ cm^{-1}; $H = -JS_M S_{imvd}$) and an AF intermolecular interaction ($J_{Mn}' = -12.6$ cm^{-1} and $J_{Ni}' = -4.3$ cm^{-1}) related to imidazole−oxoverdazyl π stacking.

Introduction

The concept of rational design by the self-assembly of appropriate building blocks has been successfully applied in the field of molecular magnetism. Networks with predictable topologies and, to some extent, properties have been synthesized.[1] The integration of magnetic molecular materials in devices depends on the enhancement of the magnetic ordering temperature. Diamagnetic ligands can lead to high ordering temperatures.[2] Nevertheless, using paramagnetic bridging ligands appears to be a more versatile strategy to enhance the exchange interaction. Up to date, few examples of two- or three-dimensional metal−radical networks have been reported.[3]

Oxoverdazyls are stable radicals. They have been shown to coordinate to metal ions.[4] In some cases, they demonstrate bridging abilities.[5] Their use for building extended structures is still limited to one-dimensional structures.[6,7] Modulation of the size and charge of the radical is a possible way to further increase the dimensionality. The steric hindrances imposed by 3-(4,6-dimethyl-2-pyrimidyl)-1,5-dimethyl-6-oxoverdazyl (pmvd•) are mainly due to the methyl groups borne by both the oxoverdazyl and the pyrimidine moieties. The former are essential for stabilizing the radical, while the latter can be removed. We therefore aim to use 3-(2′-imidazolyl)-1,5-dimethyl-6-oxoverdazyl (imvd•) as a substitute to pmvd•.

* Author to whom correspondence should be addressed. E-mail: train@ccr.jussieu.fr.
† Laboratoire de Chimie Inorganique et Matériaux Moléculaires.
‡ University of Detroit Mercy.
§ San Jose State University.

(1) (a) Clément, R.; Decurtins, S.; Gruselle, M.; Train, C. *Monatsh. Chem.* **2003**, *134*, 117. (b) Gaspar, A. B.; Ksenofontov, V.; Seredyuk, M.; Gutlich, P. *Coord. Chem. Rev.* **2005**, *249*, 2661. (c) Gruselle, M.; Train, C.; Boubekeur, K.; Gredin, P.; Ovanesyan, N. *Coord. Chem. Rev.* **2006**, *250*, 2491.
(2) (a) Ferlay, S.; Mallah, T.; Ouahes, R.; Veillet, P.; Verdaguer, M. *Nature (London)* **1995**, *378*, 701. (b) Holmes, S. M.; Girolami, G. S. *J. Am. Chem. Soc.* **1999**, *121*, 5593.
(3) (a) Inoue, K.; Imai, H.; Ghalsasi, P. S.; Kikuchi, K.; Ohba, M.; Okawa, H.; Yakhmi, J. V. *Angew Chem., Int. Ed* **2001**, *40*, 4242. (b) Luneau, D.; Rey, P. *Coord. Chem. Rev.* **2005**, *249*, 2591. (c) Tretyakov, E.; Fokin, S.; Romanenko, G.; Ikorskii, V.; Vasilevsky, S.; Ovcharenko, V. *Inorg. Chem.* **2006**, *45*, 3671.
(4) Koivisto, B. D.; Hicks, R. G. *Coord. Chem. Rev.* **2005**, *249*, 2612.
(5) Barclay, T. M.; Hicks, R. G.; Lemaire, M. T.; Thompson, L. K. *Inorg. Chem.* **2001**, *40*, 5581.
(6) Brook, D. J. R.; Lynch, V.; Conklin, B.; Fox, M. A. *J. Am. Chem. Soc.* **1997**, *119*, 5155.
(7) Pointillart, F.; Train, C.; Herson, P.; Marrot, J.; Verdaguer, M. *New J. Chem.* **2007**, *31*.

We describe hereafter the synthesis of imvd$^{\bullet}$ and its reduced form H$_3$imvd. The first steps in the synthetic uses of imvd$^{\bullet}$ as a ligand are then explored, leading to [M(hfac)$_2$(imvd$^{\bullet}$)] (M = Mn, Ni, hfac= (1,1,1,5,5,5)-hexafluoroacetylacetonate) complexes. All of the compounds have been fully structurally characterized by single-crystal X-ray diffraction. The magnetic properties of the paramagnetic compounds are described and analyzed on the basis of careful magneto-structural analysis.

Experimental Section

Synthesis. [Mn(hfac)$_2$] and imidazole-2-carboxaldehyde were used as purchased. [Ni(hfac)$_2$] and bis(1-methylhydrazide)carbonic acid were prepared according to the literature procedure,[8,9] except that for the latter benzene was replaced by dichloromethane. Standard Schlenk techniques were used to carry out reactions under an argon atmosphere. Dichloromethane was distilled from CaH$_2$ before use.

1,5-Dimethyl-3-(2′-imidazolyl)-6-oxotetrazane (H$_3$imvd). A total of 885 mg of bis(1-methylhydrazide)carbonic acid (M = 118 g mol^{-1}, n = 7.5 mmol) was dissolved in 140 mL of methanol. A suspension of 720 mg of 1-(H-imidazole)-2-carboxaldehyde (M = 96 g mol^{-1}, n = 7.5 mmol) in 200 mL of methanol heated up to 55 °C was added dropwise to this solution. Thirty minutes after the end of the addition, the reaction mixture was light yellow and suspension-free. The solution was then refluxed for 15 h. Finally, the solvent was removed by evaporation under reduced pressure to give a yellowish solid. Colorless blocks suitable for X-ray diffraction were obtained by recrystallization from a 4:1 ethyl acetate/methanol mixture. Yield: 74%. IR: 3178, 3132 (ν(N−H)), 3107, 2930 (ν(C−H)), 1610 (ν(C=O)), 1560, 1507, 1491 (ν(C=N)), 1389 (ν(C−C)) cm^{-1}. ^{1}H NMR (d^6-DMSO): 6.98 (bs, 2H, H$_{C4}$ and H$_{C5}$), 5.60 (d, 2H, J = 9.9 Hz, H$_{N1}$ and H$_{N4}$), 4.90 (t, 1H, J = 9.9 Hz, H$_{C2}$), 2.95 (s, 6H, H$_{C6}$ and H$_{C7}$) ppm. ^{13}C NMR (d^6-DMSO): 154.6 (C1), 142.4 (C3), 123 (broad, C5 and C4), 64.3 (C2), 37.4 (C6 and C7) ppm.[10]

1,5-Dimethyl-3-(2′-imidazolyl)-6-oxoverdazyl (imvd$^{\bullet}$). Condition 1. A total of 2.166 g of NaIO$_4$ (M = 213.9 g mol^{-1}, n = 10.125 mmol) in 60 mL of water was slowly added to a solution of H$_3$imvd (1.316 g, M = 196 g mol^{-1}, n = 6.71 mmol) in 40 mL of water. An immediate color change to orange and then deep red was observed. The solution was stirred for 2 h and extracted with chloroform (5 × 40 mL). The organic phase was dried over MgSO$_4$ and concentrated under reduced pressure to give a red solid. It was recrystallized from a 1:1 ethyl acetate/methanol mixture to yield 857 mg (66%) of pure imvd$^{\bullet}$·4H$_2$O. Single crystals suitable for X-ray diffraction were obtained by recrystallization in a 1:3:6 water/ethyl acetate/methanol mixture.

Condition 2. A total of 96 mg of imidazole-2-carboxaldehyde (M = 96 g mol^{-1}, 1 mmol) and 118 mg of 2,4-dimethylcarbono-bishydrazide (M = 118 g mol^{-1}, 1 mmol) were combined in 5 mL of 1:1 EtOH/H$_2$O mixture containing a single crystal of FeCl$_3$·6H$_2$O. After being stirred in the air at room temperature for 48 h, the dark red solution was evaporated to half the original volume and allowed to stand at 4 °C for 15 h. Initially, a precipitate (30 mg) containing both H$_3$imvd and imvd$^{\bullet}$ separated. After this was removed, further crystals (20 mg) of imvd$^{\bullet}$·5H$_2$O separated

over a period of 1 week at 4 °C (25% combined yield of H$_3$imvd and imvd$^{\bullet}$·5H$_2$O). Further refrigeration only deposited brown amorphous solids.

Both the tetrahydrate and pentahydrate were efflorescent and lost water upon prolonged exposure to air. IR: 3150 (ν(N−H)), 2964, 2925, 2855 (ν(C−H)), 1695 (ν(C=O)) 1559, 1540 (ν(C=N)), 1459, 1420 (ν(C−C)), 1101, 535 cm^{-1}. UV–vis: λ_{max} = 415 nm (ϵ = 2315 L mol^{-1} cm^{-1}, methanol). Anal. calcd for C$_7$H$_9$N$_4$O·1.66 H$_2$O: C, 37.66; H, 5.53; N, 37.66. Found: C, 38.02; H, 5.18; N, 37.26.

Synthesis of [M(hfac)$_2$(imvd$^{\bullet}$)] (M = Mn, Ni). Mn Derivative. A suspension of 93.8 mg of [Mn(hfac)$_2$]·2H$_2$O (M = 505 g mol^{-1}, n = 0.186 mmol) in 10 mL of heptane was refluxed. A 4 mL CH$_2$Cl$_2$ solution containing 39.8 mg of imvd$^{\bullet}$ (M = 193 g mol^{-1}, n = 0.206 mmol) was slowly and carefully added, resulting in immediate solubilization of the reaction mixture. The reflux was maintained for 30 min before evaporating the solvents under reduced pressure. The red solid residue was recrystallized by dissolution in CH$_2$Cl$_2$ and the addition of hexane. Slow evaporation (24 h) led to brown-red crystals suitable for X-ray diffraction. Yield: 41%. IR: 3159 (ν(N−H)), 2964 (ν(C−H)), 1702, 1649, 1610 (ν(C=O), 1561, 1535 (ν(C=N)), 1477 (ν(C−C)), 1259, 1214, 1148 (ν(C−F)) cm^{-1}. Anal. calcd for C$_{17}$H$_{11}$N$_6$O$_5$F$_{12}$Mn: C, 30.83; H, 1.67; N, 12.69. Found: C, 30.51; H, 1.69; N, 12.01.

The same procedure is used starting from 94.7 mg of [Ni(hfac)$_2$]·2H$_2$O (M = 509 g mol^{-1}, n = 0.186 mmol) to obtain [Ni(hfac)$_2$(imvd$^{\bullet}$)] as red crystals. Yield: 50%. IR: 3159 (ν(N−H)), 2964 (ν(C−H)), 1702, 1647, 1604 (ν(C=O), 1559, 1531 (ν(C=N)), 1483 (ν(C−C)), 1260, 1212, 1149 (ν(C−F)) cm^{-1}. Anal. calcd for C$_{17}$H$_{11}$N$_6$O$_5$F$_{12}$Ni: C, 30.66; H, 1.66; N, 12.62. Found: C, 30.26; H, 1.67; N, 11.95.

Physical Measurement. IR spectra were recorded on a Bio-Rad IRFT spectrometer as KBr pellets in the 250−4000 cm^{-1} region. UV–vis spectra were recorded between 250 and 800 nm on a UV-2101 PC Shimadzu spectrometer. Magnetization of a single-crystal sample was measured between 2 and 300 K at 0.1 T on a Quantum Design MPMS5 SQUID magnetometer and corrected for temperature-independent effects.

X-Ray Crystallography. A single crystal of each compound was selected, mounted onto a glass fiber, and transferred in a cold nitrogen gas stream (except for Mn(hfac)$_2$(imvd$^{\bullet}$)). Intensity data were collected with a Bruker-Nonius Kappa-CCD with graphite monochromated Mo Kα radiation (λ = 0.710 73 Å). Unit-cell parameter determinations, data collection strategies, and integrations were carried out with the Nonius EVAL-14 suite of programs.[11]

The structures were solved by direct methods using the Sir92, Sir97, or SHELXS97 programs[11] and refined by full-matrix least-squares methods using the SHELXL-97 software package.

All non-hydrogen atoms were refined anisotropically. Hydrogen atoms were placed at calculated positions or located on Fourrier difference map and restrained to their position.

Results and Discussion

Synthesis. The radical is synthesized in a two-step procedure. The first step is the coupling of the bis(1-methylhydrazide)carbonic acid[9] with the imidazole-2-carboxaldehyde, leading to the reduced form of the radical, H$_3$imvd.

The second step is the oxidation of H$_3$imvd by sodium periodate, leading to imvd$^{\bullet}$. The oxidation of H$_3$imvd in

(8) Caneschi, A.; Gatteschi, D.; Renard, J. P.; Rey, P.; Sessoli, R. *Inorg. Chem.* **1989**, *28*, 2940.

(9) Barr, C. L.; Chase, P. A.; Hicks, R. G.; Lemaire, M. T.; Stevens, C. L. *J. Org. Chem.* **1999**, *64*, 8893.

(10) The numbering refers to Figure 1a.

(11) Duisenberg, A. J. M.; Kroon-Batenburg, L. M. J.; Schreurs, A. M. M. *J. Appl. Crystallogr.* **2003**, *36*, 220.

Table 1. Data Collection Parameters for Structure Determination

	H$_3$imvd	imvd$^\bullet$·4H$_2$O	imvd$^\bullet$·5H$_2$O	Mn(hfac)$_2$(imvd$^\bullet$)	Ni(hfac)$_2$(imvd$^\bullet$)
T (K)	250	250	293	293	250
D_{calc} (g cm^{-3})	1.357	1.360	1.343	1.798	1.837
μ (mm^{-1})	0.099	0.115	0.116	0.674	0.942
θ range (deg)	3.05–30.03	3.26–30.00	2.77–28.32	1.62–30.00	2.67–30.01
h, k, l range	−11/11	−5/9	−8/9	−22/14	−22/22
	−12/12	−11/14	−13/13	−11/11	−11/11
	−18/18	−26/25	0/14	−25/24	−25/25
refln collected	16182	7571	14457	13914	29936
unique reflns	1455	2168	3380	7094	6981
reflns ($I > 2\sigma(I)$)	1089	1177	1988	3801	3827
number of variables	141	174	218	375	372
R_1 (all data)	0.0669	0.1276	0.1163	0.0837	0.1281
R_{w2} (all data)	0.1010	0.1472	0.228	0.1274	0.1949
R_1 ($I > 2\sigma(I)$)	0.0402	0.0565	0.0673	0.0434	0.0596
R_{w2} ($I > 2\sigma(I)$)	0.0912	0.1260	0.2045	0.0908	0.1566
goodness of fit	1.037	1.024	1.079	0.992	1.014
$\Delta\rho_{min}/\Delta\rho_{max}$ (e/Å^3)	0.190−0.176	0.201–0.211	0.942–0.488	0.845–0.560	0.838−0.631

aqueous solution with atmospheric oxygen catalyzed by a trace of Fe(III) is an alternative route. Though the yield for the second method is very low, the reaction conditions are notable for their exceptional mildness. Similar reactions have been reported for the synthesis of verdazyl metal complexes.[12] However, to our knowledge, metal-catalyzed oxidation resulting in an uncoordinated verdazyl radical has not been previously reported.

The overall yield is 60%, compared to the 6% overall yield for the seven-step synthesis leading to pmvd$^\bullet$.[9] Moreover, the solubility of imvd$^\bullet$ in water appears to be higher than 6.5×10^{-2} mol L^{-1}. The enhancement of the solubility compared to that of pmvd$^\bullet$ is due to the replacement of the methyl-substituted heterocycle by the imidazole moiety, which is able to donate hydrogen bonds.

The reactivity of imvd$^\bullet$ as a ligand was tested using the reaction with hexafluoroacetylacetonate- (hfac-) activated manganese(II) and nickel(II) developed for pyridine substituted verdazyl 1,5-dimethyl-3-(2-pyridyl)-6-oxoverdazyl, pyvd$^\bullet$.[13] The greater frequency of elongation of the C=O bond observed in the infrared spectroscopy of Mn and Ni complexes shows that the imvd$^\bullet$ radical is bonded to the metal ion. The persisting N−H elongation band demonstrates that the radical remains protonated. This latter observation is coherent with the use of aprotic solvents during the synthesis. In contrast with pmvd$^\bullet$, which acts as a bis(chelating) bridging ligand leading to dimers, imvd$^\bullet$ cannot bridge two metal ions because one nitrogen of the imidazole moiety remains protonated. As confirmed by X-ray diffraction, the products are thus monometallic compounds.

Structure Analysis. Data collection parameters for structure determination of H$_3$imvd, imvd$^\bullet$·4H$_2$O, imvd$^\bullet$·5H$_2$O, Mn(hfac)$_2$(imvd$^\bullet$), and Ni(hfac)$_2$(imvd$^\bullet$) are given in Table 1.
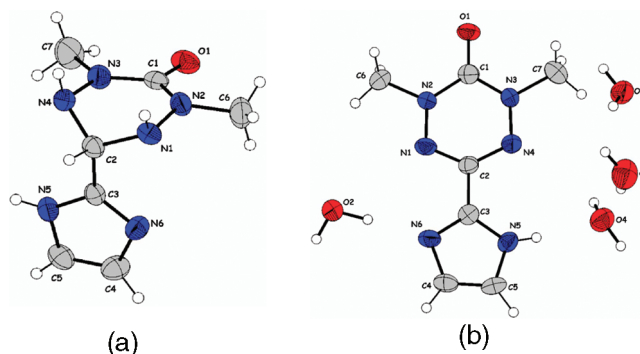
Crystal Structure of H$_3$imvd. H$_3$imvd crystallizes in the orthorhombic space group $Pca2_1$ (Table 2a). The tetrahedral geometry of the C2 atom proves the sp^3 hybridization of

(12) (a) Barclay, T. M.; Hicks, R. G.; Lemaire, M. T.; Thompson, L. K.; Xu, Z. *J. Chem. Soc., Chem. Commun.* **2002**, 1688. (b) Brook, D. J. R.; Fornell, S.; Noll, B.; Yee, G. T.; Koch, T. H. *J. Chem. Soc., Dalton. Trans.* **2000**, 2019. (c) Lemaire, M. T.; Barclay, T. M.; Thompson, L. K.; Hicks, R. G. *Inorg. Chim. Acta* **2006**, *359*, 2616.
(13) Hicks, R. G.; Lemaire, M. T.; Thompson, L. K.; Barclay, T. M. *J. Am. Chem. Soc.* **2000**, *122*, 8077.

Table 2. Crystallographic Data for H$_3$imvd and Hydrates of imvd$^\bullet$

	H$_3$imvd	imvd$^\bullet$·4H$_2$O	imvd$^\bullet$·5H$_2$O
mol mass	196.2 g mol^{-1}	265.3 g mol^{-1}	283.3 g mol^{-1}
cryst syst	orthorhombic	orthorhombic	triclinic
space group	$Pca2_1$	$P2_12_12_1$	$P\bar{1}$
a/Å	7.8564(14)	6.6408(7)	6.7838(5)
b/Å	9.1471(8)	10.4782(9)	10.4162(7)
c/Å	13.3661(16)	18.6166(18)	10.7477(7)
α/deg	90	90	83.275(4)
β/deg	90	90	71.895(4)
γ/deg	90	90	76.380(3)
vol/Å^3	960.5(2)	1295.4(2)	700.558
Z	4	4	2

this carbon atom (Figure 1a). It is confirmed by the location of H atoms on the N1, C2, and N4 atoms of the tetrazane ring. The molecule is folded with the imidazole ring and the tetrazane N−H groups, adopting an axial orientation toward the tetrazane ring. The imidazole and tetrazane planes are then nearly perpendicular, the dihedral angle between them being 83.9°. The crystal packing is fully determined by H bonding: one strong hydrogen bond links the N5−H of one molecule to the O1 of another (with an angle of 175° and an N5−O1 distance of 2.84 Å), whereas a set of two weaker hydrogen bonds exists between N1−H and N6 and N4−H and N1.

The folded geometry of this tetrazane contrasts with the one observed in the 3-(2′-pyridyl)-tetrazane analog H$_3$pyvd[14] and in its HgCl$_2$ complex[15] as well as in [Ag(I)(H$_3$pmvd)] chains[7] where the substituent of the oxoverdazyl moiety is

Figure 1. Crystal structures of H$_3$imvd (a) and imvd$^\bullet$·4H$_2$O (b).

Table 3. Selected Bond Lengths (Å) and Angles (deg) for H₃imvd and Hydrates of imvd•

	H₃imvd	imvd•·4H₂O	imvd•·5H₂O
C(1)−O(1)	1.244(3)	1.237(4)	1.234(3)
C(1)−N(2)	1.370(3)	1.373(4)	1.371(3)
C(1)−N(3)	1.359(3)	1.364(5)	1.375(3)
N(1)−N(2)	1.437(3)	1.364(4)	1.376(3)
N(3)−N(4)	1.439(3)	1.360(4)	1.360(3)
C(2)−N(1)	1.462(3)	1.320(4)	1.320(3)
C(2)−N(4)	1.465(3)	1.334(4)	1.332(3)
C(2)−C(3)	1.519(3)	1.463(4)	1.472(3)
C(3)−N(5)	1.356(3)	1.335(4)	1.348(3)
C(3)−N(6)	1.319(3)	1.330(4)	1.329(3)
C(5)−N(5)	1.379(3)	1.362(5)	1.387(3)
C(4)−N(6)	1.396(3)	1.359(5)	1.379(3)
C(5)−C(4)	1.353(3)	1.347(5)	1.348(4)
N(4)−C(2)−C(3)	111.15(16)	116.1(3)	115.9(2)
C(2)−C(3)−N(6)	126.38(18)	124.8(3)	125.8(2)

always in a pseudoequatorial orientation. On the other hand, the related imidazolium cation[16] and a 3-(2′-pyrazolyl)-tetrazane[17] show the same folded geometry. It thus appears that the presence of a H bond donor group in the molecule strongly modifies the crystal packing and favors the folded geometry.

Crystal Structures of imvd•. Two hydrates of imvd• have been identified. The number of crystallization water molecules strongly influences the space group. It is $P2_12_12_1$ for imvd•·4H₂O and $P\bar{1}$ for imvd•·5H₂O (Table 2).

Examination of the structure reveals that the verdazyl ring of the molecule is essentially planar with the C2 atom now in a triangular environment (Figure 1b). The absence of H atoms on the N1, C2, and N4 atoms also indicates that the molecule is in its oxidized form. This experimental evidence is confirmed by a complete analysis of the bond lengths and their comparison with those of H₃imvd (Table 3). The associated C2−N bond is reduced by −0.136 Å. The N−N bond is shortened by −0.076 Å. The distances in the imidazole group are also modified when going from H₃imvd to imvd•. Moreover, the two cycles constituting the imvd• molecule are not strictly coplanar. Least-squares planes for each ring are twisted along the C2−C3 axis by an angle of 13.05(16)°. This analysis confirms that, though the unpaired electron is formally borne by the N1−C2−N4 moiety, the whole molecule is deeply influenced by the oxidation process.

Within the crystal of imvd•·4H₂O, the imvd molecules are arranged in a head-to-tail manner along the 2_1 axis (Figure 2). The cycles of the neighboring molecules are parallel, separated by a mean distance of 3.415 Å and staggered by an angle of 17.54°. The crystal packing is mainly determined by the nearly planar conformation of imvd• in the solid state. The head-to-tail arrangement allows optimization of the dipolar interaction between the molecules and minimizes the steric repulsion between the methyl groups borne by the verdazyl moieties. The distance between the verdazyl and
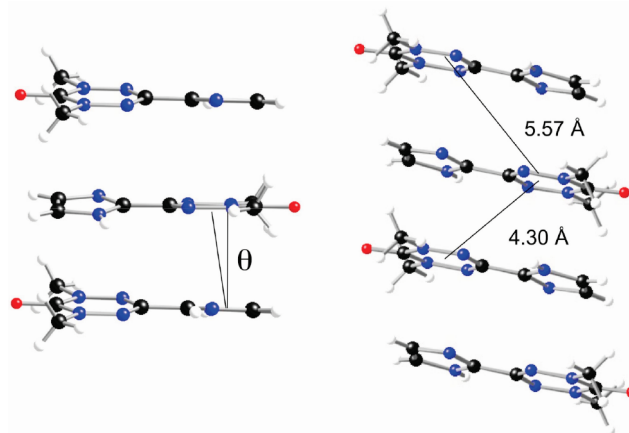
Figure 2. Crystal packing of the imvd• molecules in the tetrahydrate (left) and in the pentahydrate (right).

imidazole groups of the neighboring molecules thus becomes as low as 3.231 Å. Combined with the staggered arrangement of the cycles, this situation favors energetic stabilization of the solid state through π-orbital interaction of the neighboring molecules.[18] The stacks of radicals are separated by sheets of water molecules hydrogen-bonded to themselves and the imidazole nitrogen atoms. As a result of this segregation between water molecules and organic radicals within the crystal, the imvd• molecules form isolated chains of regularly spaced radicals. This structure is reminiscent of the hydrogen-bonded hydroquinones and free-radical stacks observed in the pyvd•−hydroquinone complex.[19]

In the pentahydrate structure, the verdazyl and imidazole rings are almost coplanar. The remaining bond distances and angles are within experimental error, the same as in the tetrahydrate. The inversion center (space group is $P\bar{1}$) creates head-to-tail stacking between two molecules separated by a distance of 3.281–3.333 Å and staggered by an angle of 10.38°. The distance between verdazyl ring centroids is then 5.57 Å. The stack with the third molecule shows a shorter distance between imidazole and verdazyl rings (3.231–3.285 Å), but the staggering angle is now 19.33° and the distance between verdazyl rings centroids is 4.30 Å. The structure of the pentahydrate itself is very similar to the tetrahydrate featuring similar head-to-tail stacks of radicals separated by sheets of water molecules. The main difference is the alternate stacking of the radicals in imvd•·5H₂O.

Crystal Structure of [(hfac)₂M(imvd•)] (M = Mn, Ni). [Mn(hfac)₂(imvd•)] and [Ni(hfac)₂(imvd•)] are isostructural (Table 4). They crystallize in the monoclinic $P2_1/c$ space group. The metal(II) ion is surrounded by six nearest neighbors: four oxygen atoms from the hfac groups and two nitrogen from the imvd• molecule. For manganese(II), three oxygen atoms of the two hfac groups are located at a mean distance of 2.139 Å, while the fourth one is as far as 2.199 Å (Table 5). The two Mn−N distances are 2.194 and 2.380 Å. The value of the C(2)−C(3)−N(6) angle is 122.2°, and

(14) Norel, L.; Chamoreau, L.-M.; Train, C. Unpublished results.

(15) Brook, D. J. R.; Fornell, S.; Stevens, J. E.; Noll, B.; Koch, T. H.; Eisfield, W. *Inorg. Chem.* **2000**, *39*, 562.

(16) Mills, A. M.; Wu, J.-Z.; Bouwman, E.; Reedijk, J.; Spek, A. L. *Acta Crystallogr., Sect. E* **2004**, *60*, o2482.

(17) Wu, J.-Z.; Bouwman, E.; Reedijk, J.; Mills, A. M.; Spek, A. L. *Inorg. Chim. Acta* **2003**, *351*, 326.

(18) Janiak, C. J. *Chem. Soc., Dalton Trans.* **2000**, 3885.

(19) Hicks, R. G.; Lemaire, M. T.; Ohrstrom, L.; Richardson, J. F.; Thompson, L. K.; Xu, Z. *J. Am. Chem. Soc.* **2001**, *123*, 7154.

**Table 4.** Crystallographic Data for [Mn(hfac)₂(imvd•)] and [Ni(hfac)₂(imvd•)]

	[Mn(hfac)₂(imvd•)]	[Ni(hfac)₂(imvd•)]
cryst syst, space group	monoclinic, $P2_1/c$	monoclinic, $P2_1/c$
mol mass	662.3 g mol⁻¹	666.0 g mol⁻¹
a/Å	16.125(3)	15.7066(19)
b/Å	8.3590(15)	8.3784(14)
c/Å	18.263(3)	18.402(2)
α/deg	90	90
β/deg	96.257(13)	95.961(9)
γ/deg	90	90
vol/Å³	2447.0(8)	2408.6(6)
Z	4	4

Table 5. Distances and Angles of [Mn(hfac)₂(imvd•)] and [Ni(hfac)₂(imvd•)] in the Crystalline State

distances/Å and angles/deg	[Mn(hfac)₂(imvd•)]	[Ni(hfac)₂(imvd•)]
M(1)−O(2)	2.199(3)	2.083(2)
M(1)−O(3)	2.140(4)	2.041(3)
M(1)−O(4)	2.134(3)	2.035(3)
M(1)−O(5)	2.144(3)	2.051(2)
M(1)−N(1)	2.380(4)	2.229(3)
M(1)−N(6)	2.194(4)	2.051(3)
N(1)−M(1)−N(6)	73.36(13)	78.02(11)
M(1)−N(1)−C(2)	112.3(3)	1181.8(2)
N(1)−C(2)−C(3)	115.2(4)	113.5(3)
C(2)−C(3)−N(6)	122.2(4)	121.3(3)
C(3)−N(6)−M(1)	115.4(3)	114.1(2)

the bite angle is 73.3°. For nickel(II), three oxygen atoms of the two hfac groups are located at a mean distance of 2.042 Å, while the fourth one is located at 2.083 Å (Table 5). The two Ni−N distances are 2.229 and 2.051 Å. The resulting octahedral geometry around the metal ion is very distorted (Figure 3). As anticipated by infrared spectroscopy, the imidazole nitrogen of imvd• remains protonated, preventing the formation of a dimer. When going from Mn(II) to Ni(II), the mean variation of the M-to-ligand distances (−0.10 Å) is in line with the variation of the ionic radius (−0.12 Å).

The difference between the two M−N(1) and M−N(6) distances can be compared to those observed in imidazolyl−pyridine or imidazolyl−pyrimidine complexes.[20] In our case, the difference between the two M−N distances is much larger.
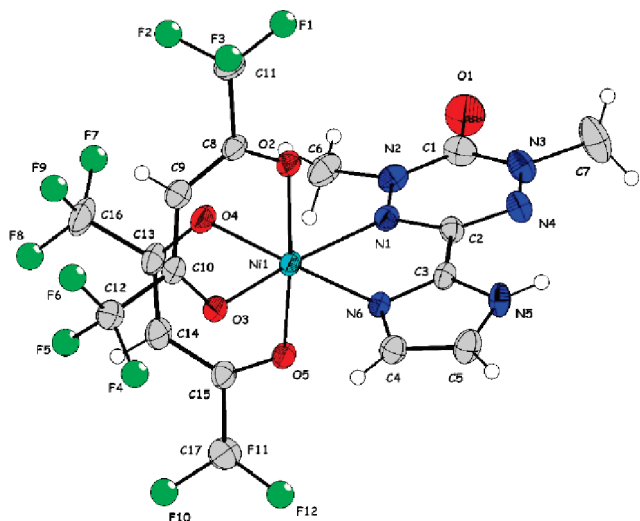
Figure 3. Ellipsoid plot of the crystal structure of [(hfac)₂Ni(imvd•)] with the numbering scheme for the atoms. The ellipsoids are shown for a 30% probability (except for fluorine atoms).
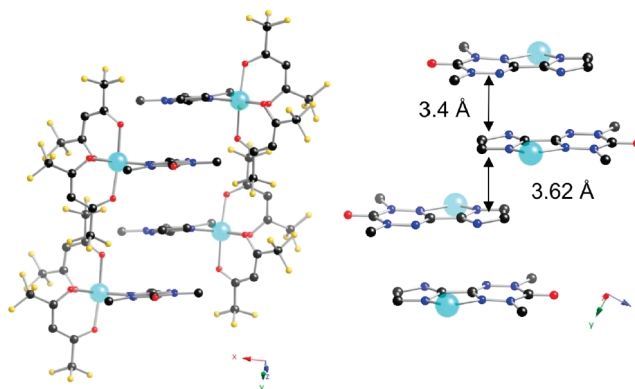
Figure 4. Stacking of [(hfac)₂Ni(imvd•)] complexes. The hfac molecules have been omitted for clarity in the right-hand picture.

This can be ascribed to both the enhanced difference in basicity between the two moieties and to the enhanced steric hindrance imposed by the methyl group of the oxoverdazyl moiety. The manganese derivatives can be compared to [(hfac)₂Mn(pmvd•)Mn(hfac)₂].[5] In the latter case, the M−X (X = O, N) distances are much more homogeneous. Once again, it appears that the reduced steric hindrance of the imidazole moiety of imvd• together with its enhanced Lewis basicity shortens the metal−imidazole bond length and weakens the metal−oxoverdazyl bond. Finally, the increase of the C(2)−C(3)−N(6) angle and the ligand bite angle is related to the substitution of the six-membered pyrimidine ring with the five-membered imidazole ring.

The crystal packing of [M(hfac)₂(imvd•)] is shown in Figure 4 for the nickel(II) derivative. The molecule itself is chiral, but in the $P2_1/c$ space group, the two enantiomers are present in the crystal, leading to the formation of a racemate. The complexes are stacked in order to favor the intermolecular interactions between the planar imvd• ligand on one side and the CF₃ moieties of the hfac groups on the other. The molecular arrangement is such that the hfac groups and the aromatic cycles segregate from one another to favor polyphilic-like interactions.[21]

Along the chains, the π stacking of the radicals is rather complex (Figure 4). It must be finely analyzed because it can strongly influence the magnetic properties of such compounds.[19,22] Two different kinds of stacking between imvd• molecules alternate along the chains. The first one corresponds to oxoverdazyl/imidazole stacking in the 3.421–3.475 Å range. The second one is imidazole/imidazole stacking separated by 3.622 Å. As far as spin bearers are concerned, the structure can thus be described as two metal−radical complexes associated into dimeric units, the dimers being themselves associated through the imidazole/imidazole stacking.

(20) (a) Mishra, H.; Mukherjee, R. J. Organomet. Chem. **2006**, 691, 3545. (b) Rodriguez, A.; Kivekas, R.; Colacio, E. J. Chem. Soc., Chem. Commun. **2005**, 5228.
(21) Tournilhac, F. G.; Bosio, L.; Bourgoin, J. P.; Vandevyver, M. J. Phys. Chem. **1994**, 98, 4870.
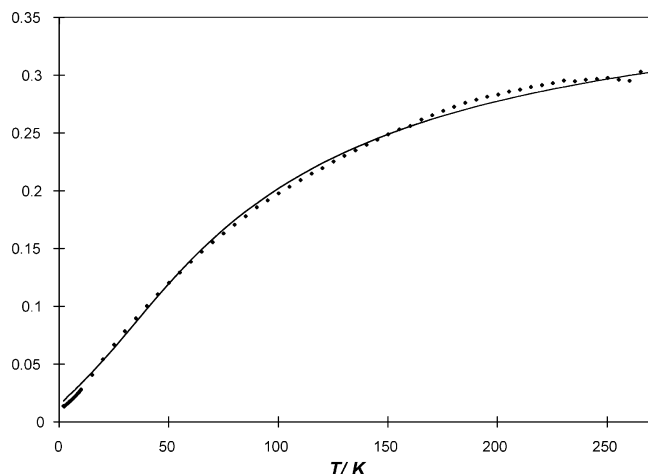(22) Meyer, A.; Gleizes, A.; Girerd, J. J.; Verdaguer, M.; Kahn, O. Inorg. Chem. **1982**, 21, 1729.

Figure 5. Thermal variation of the $\chi_M T$ product for imvd$^•$ The solid line is a fit to the linear Heisenberg model of Smith and Friedman with $J = -100$ cm^{-1} assuming a complete loss of solvate from the structure.

Magnetic Properties. Magnetic Properties of imvd$^•$. Magnetic data for imvd$^•$ are shown in Figure 5. Though the initial sample was the tetrahydrate, the sample almost certainly lost water. In fact the data are consistent with a complete loss of the solvate. Because of the loss of solvent, the crystal packing in this sample is uncertain. Nevertheless, certain features are worth noting. Below 270 K, the product $\chi_M T$ decreases markedly with decreasing temperature. A small "Curie tail" is seen at low temperatures, which is probably a result of residual uncoupled spins.[22] The whole shape of the curve agrees with an antiferromagnetic (AF) interaction between spin carriers. Considering the original π-stacked structure of the hydrates, the magnetic data can be fitted to the one-dimensional Heisenberg chain model of Smith and Friedberg[23] with an antiferromagnetic coupling constant of -100 cm^{-1} ($H = -J\sum S_i S_{i+1}$). The fit is reasonable, suggesting that the π-stacked structure is maintained. The antiferromagnetic coupling is similar in magnitude to that observed for the 3-(2$'$-pyridyl)verdazyl-hydroquinone complex.[19] As noted above, both structures feature head-to-tail π-stacked radicals separated by 3.37–3.45 Å for the hydroquinone adduct and between 3.23 and 3.333 Å for imvd$^•$·4H$_2$O.[19] If the observed antiferromagnetic coupling is a result of π stacking, it results from the overlap between the SOMO orbitals. Even though the spin density is mainly located on the verdazyl ring, residual spin density must exist on the imidazole ring as it exists on the pyridine ring of pyvd$^•$.[24] The large value of the intermolecular coupling is at first surprising, but it is noteworthy that intermolecular J couplings of over -2000 cm^{-1} have been reported for the 1,1$'$-bis(verdazyl)ferrocene diradical where the two verdazyls are eclipsed one over the other and separated by 3.15 Å, favoring a much larger overlap between the SOMOs.[25]

Magnetic Properties of [M(hfac)$_2$(imvd$^•$)] (M = Mn, Ni). We have performed magnetic measurements on the [M(hfac)$_2$(imvd$^•$)] (M = Mn, Ni) compounds. For the manganese(II) complex, upon cooling, the $\chi_M T$ curve shows a monotonic decrease from 4.1 cm^3 K mol^{-1} at 300 K (Figure 6). The decrease rate slowly increases down to 100 K. At 50 K, an inflection is observed. Finally, the $\chi_M T$ product shows a marked decrease down to 5 K. For the nickel(II) compound, upon cooling, the $\chi_M T$ curve increases from 1.8 cm^3 K mol^{-1} at 300 K to reach a round maximum at 75 K, where $\chi_M T$ is equal to 1.95 cm^3 K mol^{-1} (Figure 6). Upon further cooling, the $\chi_M T$ product drops off with an increasing rate down to 5 K.

For the manganese(II) derivative, the $\chi_M T$ value at 300 K is lower than the 4.75 cm^3 K mol^{-1} value expected for independent paramagnetic radical ($S_{imvd} = 1/2$, $g = 2$) and Mn(II) ($S_{Mn} = 5/2$, $g = 2$) ion. The thermal evolution of $\chi_M T$ is characteristic of an AF coupling between the spin carriers, justifying the low value of $\chi_M T$ at ambient temperatures. The general shape of the curve down to 50 K is in accordance with what can be expected from an assembly of independent strongly antiferromagnetically coupled (S_{imvd}, S_{Mn}) systems. For the nickel(II) derivative, the $\chi_M T$ value at 300 K is much higher than the 1.48 cm^3 K mol^{-1} value expected for an independent paramagnetic radical ($S_{imvd} = 1/2$, $g = 2$) and Ni(II) ($S_{Ni} = 1$, $g = 2.1$) ion. The thermal evolution of $\chi_M T$ is characteristic of a strong ferromagnetic (F) coupling between the spin carriers, justifying the high value of $\chi_M T$ at ambient temperatures. The general shape of the curve down to 75 K is in accordance with what can be expected from an assembly of independent strongly ferromagnetically coupled (S_{imvd}, S_{Ni}) systems. In both cases, the steep decrease at low temperatures is indicative of an additional antiferromagnetic interaction between the [M(hfac)$_2$(imvd$^•$)] complexes. Following this analysis, the high-temperature region has been fitted using a classical dimer law, setting the g value of the radical to 2.0.[26] The agreement between the experimental values and the calculated ones is excellent. For the manganese(II) derivatives, the values deduced from the fit are $J = -65$ cm^{-1} ($H = -J S_{imvd} S_M$) and $g_{Mn} = 2.03$. For the nickel(II) derivatives, the values deduced from the fit are $J = +195$ cm^{-1} and $g_{Ni} = 2.10$.

For both compounds, the fit of the curve on the whole temperature range can be done by treating the antiferromagnetic interaction between the (S_{imvd}, S_M) systems. As anticipated by the analysis of the crystal packing in both Mn and Ni compounds (Figure 6), the data cannot be fitted by a regular chain model. The association of metal–radical complexes into dimeric units by imidazole/oxoverdazyl stacking must lead to significant antiferromagnetic coupling, J', between them,[19,25] while negligible interaction is mediated by imidazole/imidazole stacking between the dimers. We thus considered a four-spin system (S_M, S_{imvd}, S_{imvd}, S_M) with two coupling constants J and J' for fitting the magnetic data (Figure 7). Because no analytical

(23) Smith, T.; Friedberg, S. A. *Phys. Rev.* **1968**, *176*, 660.
(24) Jornet, J.; Deumal, M.; Ribas-Arino, J.; Bearpark, M. J.; Robb, M. A.; Hicks, R. G.; Novoa, J. J. *Chem.—Eur. J.* **2006**, *12*, 3995.
(25) Koivisto, B. D.; Ichimura, A. S.; McDonald, R.; Lemaire, M. T.; Thompson, L. K.; Hicks, R. G. *J. Am. Chem. Soc.* **2006**, *128*, 690.
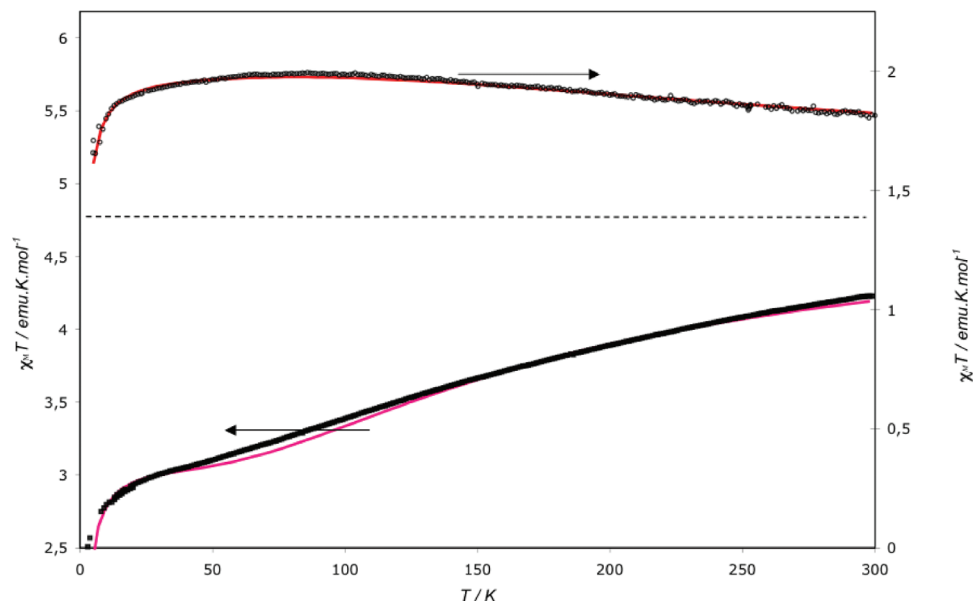(26) Kahn, O. *Molecular Magnetism*; Wiley-VCH Verlag GmbH: Weinheim, Germany, 1993.

Figure 6. Thermal variation of the $\chi_M T$ product measured in a 0.5 T applied field for [Mn(hfac)$_2$(imvd$^\bullet$)] (lower plots) and [Ni(hfac)$_2$(imvd$^\bullet$)] (upper plots). The fits (see text) are shown as solid lines. The dashed line represents the expected values for isolated spins.
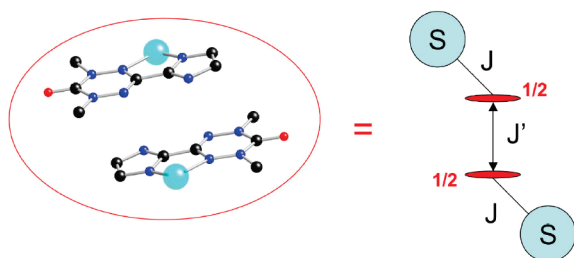

Figure 7. Four-spin system considered for fitting the magnetic behaviors associated with complexes' dimerization (hfac molecules are omitted for clarity).

expression can be derived for such systems, the fitting has been performed by full-matrix diagonalization of the appropriate spin Hamiltonian:

$$H = -J(S_{M1}S_{imvd1} + S_{M2}S_{imvd2}) - J'S_{imvd1}S_{imvd2} + g_M\beta(S_{M1} + S_{M2})B + g_{imvd}\beta(S_{imvd1} + S_{imvd2})B$$

The Nelder Mead algorithm has been used with the Mathematica software. When the g values are fixed and the J values deduced from the high-temperature analysis are started from, this fitting procedure gives $J = -62.5$ cm^{-1} and $J' = -12.6$ cm^{-1} for the Mn derivative and $J = +193$ cm^{-1} and $J' = -4.31$ cm^{-1} for the Ni derivative. The fit is very good for the Ni complex but partly failed to fully reproduce the inflection region of the thermal variation of the $\chi_M T$ of the Mn derivative. Nevertheless, this fitting procedure led to better results than the one previously described for a comparable four-spin system.[27]

As far as the metal–radical exchange interaction is concerned, our results are in agreement with previous studies in the literature. For the [M(hfac)$_2$(pyvd$^\bullet$)] (M = Ni, Mn) complexes, the coupling constants determined are -45 cm^{-1} for the Mn derivative and $+240$ cm^{-1} for the Ni derivative.

Those found for the [(hfac)$_2$M(pmvd$^\bullet$)M(hfac)$_2$] (M = Mn, Ni) compounds[5] are, respectively, -48 and $+220$ cm^{-1}. In the present case, absolute values are 25% larger for Mn(II) and slightly lower for Ni(II).

The radical–radical interaction, J', certainly depends on the overlap between the SOMOs of the radicals.[24] It is thus sensitive to three factors: (a) the nature of the cycles that face one another ranging from very weak for imidazole−imidazole stacking, intermediate for imidazole−verdazyl stacking, to very strong for verdazyl−verdazyl stacking;[25] (b) the distance and angle between the cycles; and (c) the spin density on the cycles. In Mn and Ni complexes, distances (and angles) between the radical planes are less favorable than in imvd$^\bullet$·4H$_2$O; the coupling is thus smaller. When going from Ni to Mn, both b and c factors can vary so that the absolute J' value is almost 3 times greater for the Mn derivative.

Conclusion

Along these lines, we described the synthesis of an imidazole-substituted oxoverdazyl radical as well as its reduced tetrazane form. The radical has been used as a bidentate ligand toward metal ions activated by the electron-withdrawing hfac ligand to synthesize [M(hfac)$_2$(imvd$^\bullet$)] (M = Mn, Ni) complexes. These species exhibit strong intramolecular exchange interactions perceptible up to room temperature. Additional AF intermolecular interactions governed by the π stacking of the molecules and by the nature of the metal ion are observed at low temperatures.

Compared to the use of pmvd$^\bullet$ as a bridging ligand,[4–6] imvd$^\bullet$ offers (i) reduced steric hindrance, (ii) potential bridging ability upon deprotonation of the imidazole group, and (iii) stepwise construction of the desired compound through controlled deprotonation of this group. The deprotonation of the imidazole moiety of the [M(hfac)$_2$(imvd$^\bullet$)] complexes will be undertaken to explore the possibility of synthesizing systems with three different

(27) Gilroy, J. B.; Koivisto, B. D.; McDonald, R.; Ferguson, M. J.; Hicks, R. G. *J. Mater. Chem.* **2006**, *16*, 2618.

spin bearers. Such a possibility has been already reported for the 3d4f3d′ system.[28] Using $[M(hfac)_2(imvd^•)]$ complexes as a starting building block, it could be extended to 3d2p3d′ or 3d2p4f. Such species are very appealing for the development of multifunctionality at the molecular level.

Note Added after ASAP Publication. This article was released ASAP on March 5, 2008, with a missing Supporting Information paragraph. The correct version was posted on March 31, 2008.

Supporting Information Available: X-ray crystallographic data in CIF format. This material is available free of charge via the Internet at http://pubs.acs.org.

IC701400B

(28) Gheorghe, R.; Andruh, M.; Costes, J. P.; Donnadieu, B. *J. Chem. Soc., Chem. Commun.* **2003**, 2778.